Fast communication

Ψ_B-energy operator and cross-power spectral density

Abdel-Ouahab Boudraa [a,*], Thierry Chonavel [b], Jean-Christophe Cexus [c]

[a] IRENav, Ecole Navale, BCRM Brest, CC 600, 29240 Brest Cedex 9, France
[b] Lab-Sticc, Télécom Bretagne, Technopole Brest-Iroise, 29238 Brest Cedex 3, France
[c] Lab-Sticc, ENSTA-Bretagne, 2 rue François Verny, 29806 Brest, France

A B S T R A C T

In this paper we consider the hermitian extension of the cross-Ψ_B-energy operator that we will denote by Ψ_H. In addition, cross energy terms are formalized through multivariate signals representation. We investigate the connection between the interaction energy function of Ψ_H and the cross-power spectral density (CPSD) of two complex valued signals. In particular, this link permits to use this operator for estimating the CPSD. We illustrate the interest of Ψ_H as a similarity between a pair of signals in frequency domain on synthetic and real data.

Keywords:
Ψ_H-energy operator
Cross-Ψ_B-energy operator
Teager–Kaiser energy operator
Cross-power spectral density

1. Introduction

Since its introduction, the cross-Ψ_B-energy operator [1] has been used in different domains, including time series analysis [2], gene time series expression data clustering [3], wave equation [4], transient detection [5], time delay estimation [6] or time–frequency analysis [7]. These applications show that Ψ_B, which is a complex and symmetric version of the cross-Teager–Kaiser energy operator [8], is well suited for processing of non-stationary signals.

In this paper, we introduce an hermitian version of Ψ_B that we denote by Ψ_H. In particular, it contains all the information in Ψ_B and has a more compact expression. In addition, its hermitian structure makes it quite natural for handling complex signals. Then, we establish the connection between Ψ_H and the cross-power spectral density (CPSD). This function is a fundamental and powerful tool to investigate an unknown second order relationship between two signals (or time series) in the frequency domain [9]. This connection involves an interesting relationship and a simple way to estimate the CPSD and its second order power moment. Note that all the results presented here for Ψ_H also hold for Ψ_B.

2. Cross spectral density and Ψ_H operator

For two complex-valued signals x_t and y_t, Ψ_B operator is defined as follows [1]:

$$\Psi_B[x_t,y_t]=\frac{1}{2}[\dot{x}_t^*\dot{y}_t+\dot{x}_t\dot{y}_t^*]-\frac{1}{4}[x_t\ddot{y}_t^*+x_t^*\ddot{y}_t+y_t\ddot{x}_t^*+y_t^*\ddot{x}_t] \quad (1)$$

where .* denotes complex conjugation. Alternatively, we define the Ψ_H operator as

$$\Psi_H[x_t,y_t]=\dot{x}_t\dot{y}_t^*-\frac{1}{2}[x_t\ddot{y}_t^*+\ddot{x}_t y_t^*]. \quad (2)$$

Clearly $\Psi_H[y_t,x_t]=\Psi_H^*[x_t,y_t]$ and $\Psi_B[x_t,y_t]=\mathrm{Re}\{\Psi_H[x_t,y_t]\}$, where $\mathrm{Re}\{\cdot\}$ denotes the real part. Both Ψ_B and Ψ_H quantify the strength of coupling or interaction between x_t and y_t.

We also introduce the following multivariate extension of the energy operator: letting $\mathbf{z}_1$ and $\mathbf{z}_2$ denote two

* Corresponding author. Tel.: +33 2 98 23 40 37; fax: +33 2 98 23 38 57.
E-mail address: boudra@ecole-navale.fr (A.-O. Boudraa).

complex valued vector functions defined on $\mathbb{R}$, we let

$$\Psi_{\mathrm{H}}[\mathbf{z}_{1t},\mathbf{z}_{2t}]=\dot{\mathbf{z}}_{1t}\dot{\mathbf{z}}_{2t}^{H}-\frac{1}{2}[\mathbf{z}_{1t}\ddot{\mathbf{z}}_{2t}^{H}+\ddot{\mathbf{z}}_{1t}\mathbf{z}_{2t}^{H}] \tag{3}$$

where $.^{H}$ denotes hermitian conjugation, that is, transposition plus conjugation. In particular, when $\mathbf{z}_1=\mathbf{z}_2=\mathbf{z}$, with $\mathbf{z}=[x,y]^T$, we get

$$\Psi_{\mathrm{H}}[\mathbf{z}_t,\mathbf{z}_t]=\begin{bmatrix}\Psi_{\mathrm{H}}[x_t,x_t] & \Psi_{\mathrm{H}}[x_t,y_t]\\ \Psi_{\mathrm{H}}[y_t,x_t] & \Psi_{\mathrm{H}}[y_t,y_t]\end{bmatrix} \tag{4}$$

The cross terms in the matrix $\Psi_{\mathrm{H}}[\mathbf{z}_t,\mathbf{z}_t]$ measure the coupling between x_t and y_t at time t.

The averaged Ψ_{B} interaction energy has been defined in [6] for finite energy signals. It follows that we can similarly define, for finite power signals, the multivariate average interaction for Ψ_{H} in terms of time average as

$$\mathrm{E}_{\mathrm{H}\mathbf{z}_1\mathbf{z}_2}(\tau)=\lim_{T\to\infty}\frac{1}{2T}\int_{-T}^{T}\Psi_{\mathrm{H}}[\mathbf{z}_{1t},\mathbf{z}_{2,t-\tau}]\,dt. \tag{5}$$

Function $\mathrm{E}_{\mathrm{H}\mathbf{z}_1\mathbf{z}_2}(\tau)$ measures how similar $\mathbf{z}_1$ and $\mathbf{z}_2$ are at lag τ.

As before, letting $\mathbf{z}_1=\mathbf{z}_2=\mathbf{z}$, with $\mathbf{z}=[x,y]^T$, we get the matrix expression of $\mathrm{E}_{\mathrm{H}\ \mathbf{zz}}(\tau)$ in the form

$$\mathrm{E}_{\mathrm{H}\mathbf{zz}}(\tau)=\begin{bmatrix}\mathrm{E}_{\mathrm{H}xx}(\tau) & \mathrm{E}_{\mathrm{H}xy}(\tau)\\ \mathrm{E}_{\mathrm{H}yx}(\tau) & \mathrm{E}_{\mathrm{H}yy}(\tau)\end{bmatrix}. \tag{6}$$

In particular, the cross-interaction between x and y is defined by

$$\mathrm{E}_{\mathrm{H}xy}(\tau)=\lim_{T\to\infty}\frac{1}{2T}\int_{-T}^{T}\Psi_{\mathrm{H}}[x_t,y_{t-\tau}]\,dt. \tag{7}$$

$\mathrm{E}_{\mathrm{H}xy}(\tau)$ quantifies the average coupling between x_t and the delayed signal $y_{t-\tau}$.

In the following, we are going to highlight the relationship between E_{H} and the correlation function. The cross-correlation between multivariate signals $\mathbf{z}_1$ and $\mathbf{z}_2$ is defined by

$$R_{\mathbf{z}_1\mathbf{z}_2}(\tau)=\lim_{T\to\infty}\frac{1}{2T}\int_{-T}^{T}\mathbf{z}_{1t}\mathbf{z}_{2,t-\tau}^{H}\,dt. \tag{8}$$

Thus, for $\mathbf{z}_1=\mathbf{z}_2=\mathbf{z}=[x,y]^T$ we have

$$R_{\mathbf{zz}}(\tau)=\begin{bmatrix}R_{xx}(\tau) & R_{xy}(\tau)\\ R_{yx}(\tau) & R_{yy}(\tau)\end{bmatrix}. \tag{9}$$

Note that $R_{yx}(\tau)=R_{xy}^{*}(-\tau)$.

Now, let us recall the following straightforward property: for two positive integers l and m, we have

$$\frac{\partial^{l+m}}{\partial\tau^{l+m}}R_{\mathbf{z}_1\mathbf{z}_2}(\tau)=(-1)^{(m)}R_{\mathbf{z}_1^{(l)}\mathbf{z}_2^{(m)}}(\tau) \tag{10}$$

where $\mathbf{z}^{(m)}$ is the mth derivative of $\mathbf{z}$. For conciseness $\mathbf{z}^{(1)}$ and $\mathbf{z}^{(2)}$ are simply denoted by $\dot{\mathbf{z}}$ and $\ddot{\mathbf{z}}$ as above. Then, we can state that

Proposition 1.

$$\mathrm{E}_{\mathrm{H}\mathbf{z}_1\mathbf{z}_2}(\tau)=2R_{\dot{\mathbf{z}}_1\dot{\mathbf{z}}_2}(\tau) \tag{11}$$

In particular, for scalar signals x and y, we get $\mathrm{E}_{\mathrm{H}xy}(\tau)=2R_{\dot{x}\dot{y}}(\tau)$.

Proof. Using relation (10), we get

$$\begin{aligned}\mathrm{E}_{\mathrm{H}\mathbf{z}_1\mathbf{z}_2}(\tau)&=\lim_{T\to\infty}\frac{1}{2T}\int_{-T}^{T}\dot{\mathbf{z}}_{1t}\dot{\mathbf{z}}_{2,t-\tau}^{H}\\ &\quad-\frac{1}{2}[\ddot{\mathbf{z}}_{1t}\mathbf{z}_{2,t-\tau}^{H}+\mathbf{z}_{1t}\ddot{\mathbf{z}}_{2,t-\tau}^{H}]\,dt.\\ &=R_{\dot{\mathbf{z}}_1\dot{\mathbf{z}}_2}(\tau)-\frac{1}{2}[R_{\ddot{\mathbf{z}}_1\mathbf{z}_2}(\tau)+R_{\mathbf{z}_1\ddot{\mathbf{z}}_2}(\tau)]\\ &=2R_{\dot{\mathbf{z}}_1\dot{\mathbf{z}}_2}(\tau)\qquad\square\end{aligned} \tag{12}$$

The cross-spectrum density of $\mathbf{z}_1$ and $\mathbf{z}_2$ will be denoted by $S_{\mathbf{z}_1\mathbf{z}_2}$. It is defined as the Fourier transform of $R_{\mathbf{z}_1\mathbf{z}_2}(\tau)$: $S_{\mathbf{z}_1\mathbf{z}_2}(f)=\mathcal{F}[R_{\mathbf{z}_1\mathbf{z}_2}(\tau)]$. In particular, for $\mathbf{z}_1=\mathbf{z}_2=\mathbf{z}=[x,y]^T$, we get

$$S_{\mathbf{zz}}(f)=\begin{bmatrix}S_{xx}(f) & S_{xy}(f)\\ S_{yx}(f) & S_{yy}(f)\end{bmatrix} \tag{13}$$

where it is clear that $S_{yx}(f)=S_{xy}^{*}(f)$, since $R_{yx}(\tau)=R_{xy}^{*}(-\tau)$. Then, we get the following result:

Proposition 2.

$$\mathcal{F}[\mathrm{E}_{\mathrm{H}\mathbf{z}_1\mathbf{z}_2}(\tau)]=2S_{\dot{\mathbf{z}}_1\dot{\mathbf{z}}_2}(f) \tag{14}$$

In particular, for scalar signals x and y, we get $\mathcal{F}[\mathrm{E}_{\mathrm{H}xy}(\tau)]=2S_{\dot{x}\dot{y}}(f)$.

Proof. From Proposition 1, $\mathrm{E}_{\mathrm{H}\mathbf{z}_1\mathbf{z}_2}(\tau)=2R_{\dot{\mathbf{z}}_1\dot{\mathbf{z}}_2}(\tau)$. Then, $\mathcal{F}[\mathrm{E}_{\mathrm{H}\mathbf{z}_1\mathbf{z}_2}(\tau)]=2\mathcal{F}[R_{\dot{\mathbf{z}}_1\dot{\mathbf{z}}_2}(\tau)]=2S_{\dot{\mathbf{z}}_1\dot{\mathbf{z}}_2}(f)$. □

It is well known that the derivation operator amounts to a filtering operation by a filter with frequency response $\hat{h}(f)=2i\pi f$. Then, for a scalar signal x, we get $\mathcal{F}[\dot{x}]=\hat{h}(f)\,\mathcal{F}[x]$. More generally, if $\mathbf{z}_1$ and $\mathbf{z}_2$ are $\mathbb{C}^n$ valued complex signals we obtain

$$\mathcal{F}\begin{bmatrix}\dot{\mathbf{z}}_1\\ \dot{\mathbf{z}}_2\end{bmatrix}=\hat{h}(f)\times\mathcal{F}\begin{bmatrix}\mathbf{z}_1\\ \mathbf{z}_2\end{bmatrix} \tag{15}$$

Then, the average interaction $\mathrm{E}_{\mathrm{H}\mathbf{z}_1\mathbf{z}_2}$ can be expressed from the cross spectrum $S_{\mathbf{z}_1\mathbf{z}_2}$ as follows:

Proposition 3.

$$\mathrm{E}_{\mathrm{H}\mathbf{z}_1\mathbf{z}_2}(\tau)=8\pi^2\int_{\mathbb{R}}f^2S_{\mathbf{z}_1\mathbf{z}_2}(f)e^{2j\pi f\tau}\,df \tag{16}$$

In particular, for scalar signals x and y, we get the expression of $\mathrm{E}_{\mathrm{H}xy}(\tau)$ *in terms of the cross-spectrum of x and y*:

$$\mathrm{E}_{\mathrm{H}xy}(\tau)=8\pi^2\int_{\mathbb{R}}f^2S_{xy}(f)e^{2j\pi f\tau}\,df \tag{17}$$

Proof. From Eqs. (14) and (15), we get

$$\begin{aligned}S_{\dot{\mathbf{z}}_1\dot{\mathbf{z}}_2}(f)&=|\hat{h}(f)|^2S_{\mathbf{z}_1\mathbf{z}_2}(f)\\ &=\frac{1}{2}\mathcal{F}[\mathrm{E}_{\mathrm{H}\mathbf{z}_1\mathbf{z}_2}(\tau)]\end{aligned} \tag{18}$$

Then, applying the inverse Fourier transform in the above equation yields

$$\begin{aligned}\mathrm{E}_{\mathrm{H}\mathbf{z}_1\mathbf{z}_2}(\tau)&=2\int_{\mathbb{R}}|\hat{h}(f)|^2S_{\mathbf{z}_1\mathbf{z}_2}(f)e^{2j\pi f\tau}\,df\\ &=8\pi^2\int_{\mathbb{R}}f^2S_{\mathbf{z}_1\mathbf{z}_2}(f)e^{2j\pi f\tau}\,df\qquad\square\end{aligned} \tag{19}$$

Note that, up to the constant factor $8\pi^2$, $\mathrm{E}_{\mathrm{H}\mathbf{z}_1\mathbf{z}_2}(\tau)$ is the second order power moment of $S_{\mathbf{z}_1\mathbf{z}_2}(f)$. Also, relation (18) yields

$$S_{xy}(f) = (8\pi^2 f^2)^{-1}\mathcal{F}[\mathrm{E}_{\mathrm{H}xy}(\tau)] \tag{20}$$

This relation suggests possible use of $\mathrm{E}_{\mathrm{H}xy}(\tau)$ for CPSD estimation purpose. In particular, the spectral coherence function between two real valued stationary zeros mean signals x_t and y_t is a normalized version of the cross power spectral density $S_{xy}(f)$ defined as

$$\gamma^{S}_{xy}(f) = \frac{|S_{xy}(f)|}{\sqrt{S_{xx}(f)}\cdot\sqrt{S_{yy}(f)}}. \tag{21}$$

$\gamma^{\mathbb{S}}_{xy}(f)$ takes its values in [0,1]. It is interesting to measure the correlation among x and y, up to a possible filtering. Indeed, it is straightforward that $\gamma^{\mathbb{S}}_{xy}(f)$ is left unchanged through invertible filtering of x or y which is replaced by a filtered version of itself. Clearly, from (20) $\gamma^{H}_{xy}(f)$ can be rewritten as

$$\gamma^{H}_{xy}(f) = \frac{|\mathcal{F}[\mathrm{E}_{\mathrm{H}xy}](f)|}{\sqrt{\mathcal{F}[\mathrm{E}_{\mathrm{H}xx}](f)}\cdot\sqrt{\mathcal{F}[\mathrm{E}_{\mathrm{H}yy}](f)}}. \tag{22}$$

Note that since $(\gamma^{H}_{xy}(f))^2 \leq 1$, $|\mathcal{F}[\mathrm{E}_{\mathrm{H}xy}](f)|^2 \leq \mathcal{F}[\mathrm{E}_{\mathrm{H}xx}](f)\cdot\mathcal{F}[\mathrm{E}_{\mathrm{H}yy}](f)$.

When $\mathcal{F}[\mathrm{E}_{\mathrm{H}xy}](f)$ is equal to zero, x_t and y_t are uncorrelated at frequency f. At the opposite if $\mathcal{F}[\mathrm{E}_{\mathrm{H}xy}](f)$ is equal to 1, x_t and y_t are fully correlated.

3. Results

In this section an application of Ψ_{H} for non-stationary signal analysis is presented. We show the efficiency of γ^{H}_{xy} to estimate similarity between a signal and its noisy filtered version in the frequency domain. Let x_t be some known (AM–FM) signal

$$\begin{aligned} x_t &= a_t e^{j\phi(t)} \\ a_t &= 1+\kappa\cos(\omega_a t) \\ \phi(t) &= \left(\omega_c t + \omega_m \int_0^t q_\tau\, d\tau\right) \\ q_t &= \sin(\omega_q t) \end{aligned} \tag{23}$$

where a_t is the time-varying amplitude, ω_c the carrier frequency, κ the AM modulation index, q_t the frequency modulating signal and ω_m the maximum frequency deviation. For simulation, the parameter values used are $\omega_q = 0.63$, $\omega_a = 0.63$, $\omega_c = 1.57$, $\omega_m = 0.94$ and $\kappa = 0.7$. Let y_t denote the observed signal. y_t is a noisy filtered version of x_t, where the filter impulse response is denoted by g_t:

$$y_t = (g * x)_t + n_t \tag{24}$$

The additive noise n_t is a complex circularly white Gaussian noise. For the transfer function of the filter we choose

$$G(z) = 1 + \sum_{k=1}^{L-1} g_k z^{-k} \tag{25}$$

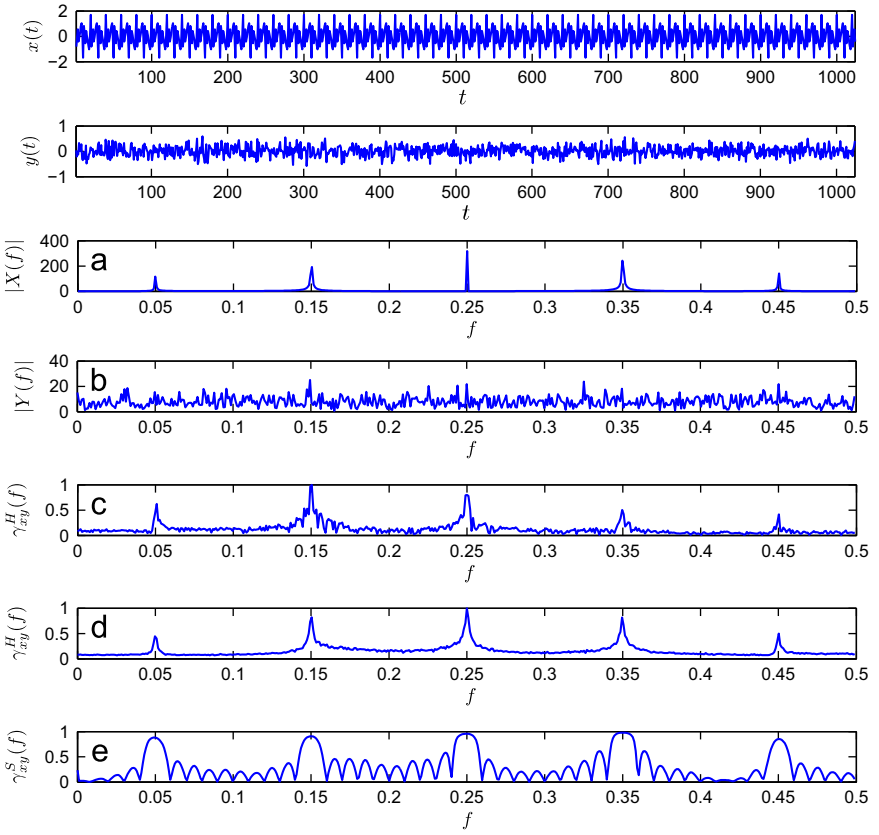

Fig. 1. Analysis of AM–FM signals.

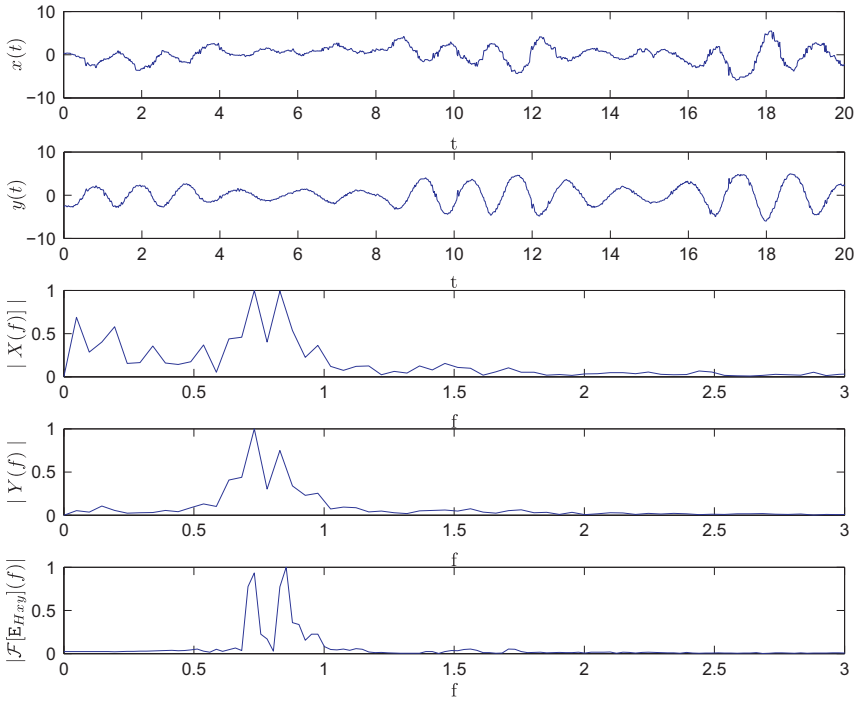

Fig. 2. Analysis of aerodynamic signals.

with $g_k \sim 0.1 \times \mathcal{N}(0,1)$ and $L=10$. The signal to noise ratio is set to 0 dB that is the mean power of $g*x$ is equal to that of the noise n. To detect the presence of filtered x_t in y_t a spectral coherence function given by Eq. (21) or Eq. (22) can be used. The spectra $\mathcal{F}[\mathrm{E}_{\mathrm{H}xx}(\tau)]$ and $\mathcal{F}[\mathrm{E}_{\mathrm{H}yy}(\tau)]$ of x_t and y_t and their cross spectrum $\mathcal{F}[\mathrm{E}_{\mathrm{H}xy}(\tau)]$ can be derived from the discrete Fourier transform. Applying Eq. (22) involves the derivation of y_t. When n_t is a white noise, the finite difference achieves poor estimation of the derivative. There are several smoothing techniques in the literature [10,11] that can be considered for derivating signals that are corrupted by white noise. The definition of E_{H} in Eq. (5) involves the computation of Ψ_{H}, and thus derivatives, but integration compensates for above mentioned difficulties and we do not need to apply sophisticated derivation techniques.

In Fig. 1(c)–(d) we plot the estimated $\gamma^H_{xy}(f)$ obtained after averaging over 1 and 20 realization of data of the experiment respectively. We can check that provided $\gamma^H_{xy}(f)$ is averaged over sufficiently many experiments, it catches well the spectral peaks of x (Fig. 1(a)) in spite of the low signal to noise ratio (Fig. 1(d)). Due to its connection with spectra it is clear that the resolution of the estimated coherence increases with the length of averaged data sets while its variance decreases as the number of data sets used for its estimation increases. As for spectral estimation, the limit to distinguish frequency peaks depends on the SNR and on the amount of data available for estimation. Compared to the corresponding averaged spectra of y (Fig. 1(b)) and $\gamma^S_{xy}(f)$ (Fig. 1(e)) we see that $\gamma^H_{xy}(f)$ achieves better spectral peaks detection since the effect of filter is removed in the calculation of coherence (Fig. 1(d)). We report in Fig. 1(e) the coherence function calculated from signals spectra. This function is calculated using the MatLab function mscohere.m with the same FFT length as for the calculation from E_{H} (Eq. (22)) and using rectangular window. Although spectrum-based calculation of coherence shows peaks that are often higher, the E_{H} based calculation shows higher resolution.

We also illustrate the interest of Ψ_{H} operator on real aerodynamic data, recorded on an instrumented yacht sailing upwind in a moderate head swell [12]. The wind signal is recorded at the top of a mast by means of a 3D acoustic anemometer that measures the instantaneous Apparent Wind Speed: $x_t = \mathrm{AWS}_{\dot{\theta}}(t)$. The boat pitch angle is denoted by $\theta(t)$. The corresponding pitch angle velocity is $\dot{\theta}(t)$. $\dot{\theta}(t)$ is recorded by a central of attitude located at the center of rotation of the boat. The pitch induces apparent wind speed $y_t = h\dot{\theta}(t)$ at the top of the mast, where h is the height of the mast. Variations of the apparent wind speed time series y_t are related to the frequency of waves along the boat trajectory. These variations are the reason for the aerodynamic performance oscillation of the sail plan when pitching. During a 20 s record (see x_t and y_t in Fig. 2), the swell has shown different periods. This results from the swell encountering waves at frequencies f_1 and f_2 equal to 0.73 Hz and 0.85 Hz respectively. We assume that x_t and y_t are ergodic processes. Frequencies f_1 and f_2 are well evidenced by $\mathcal{F}[\mathrm{E}_{\mathrm{H}xy}](f)$ (bottom plot) as common frequencies of these two signals. As it can be seen in Fig. 2, the peaks of $\mathcal{F}[\mathrm{E}_{\mathrm{H}xy}](f)$ at f_1 and f_2 show very strong correlation of x_t and y_t at these two frequencies. This confirms that Ψ_{H} is useful to show the similarities between two signals in the frequency domain.

4. Conclusion

In this paper we introduced the hermitian extension of the cross-Ψ_B-energy operator, denoted by Ψ_H. Clearly, Ψ_H supplies a framework to study cross-energy of complex-values signals that is more natural than Ψ_B. Relationship between Ψ_H and cross-power spectral density of two complex valued signals has been established. Preliminary results on synthetic and real signals have shown the interest of Ψ_H as a similarity measure between signals. In future works, it will be interesting to investigate the use of Ψ_H for some applications where cross-energy or coherence between complex-valued signals are involved.

References

[1] J.C. Cexus, A.O. Boudraa, Link between cross-Wigner distribution and cross-Teager energy operator, Electronics Letters 40 (12) (2004) 778–780.

[2] A.O. Boudraa, J.C. Cexus, M. Groussat, P. Brunagel, An energy-based similarity measure for time series, Advances in Signal Processing (2008) 8. ID 135892.

[3] W.F. Zhang, C.C. Liu, H. Yan, Clustering of temporal gene expression data by regularized spline regression an energy based similarity measure, Pattern Recognition 43 (2010) 3969–3976.

[4] J.P. Montillet, On a novel approach to decompose finite energy functions by energy operators and its application to the general wave equation, International Mathematical Forum 48 (2010) 2387–2400.

[5] A.O. Boudraa, S. Benramdane, J.C. Cexus, Th. Chonavel, Some useful properties of cross-Ψ_B-energy operator, International Journal of Electronics and Communications 63 (9) (2009) 728–735.

[6] A.O. Boudraa, J.C. Cexus, K. Abed-Meraim, Cross-Ψ_B-energy operator-based signal detection, Journal of the Acoustical Society of America 123 (6) (2008) 4283–4289.

[7] A.O. Boudraa, Relationships between Ψ_B-energy operator and some time–frequency representations, IEEE Signal Processing Letters 17 (6) (2010) 527–530.

[8] J.F. Kaiser, Some useful properties of Teager's energy operators, in: Proceedings of ICASSP, vol. 3, 1993, pp. 149–152.

[9] J.S. Bendat, Nonlinear System Techniques and Applications, John Wiley and Sons, Inc., NY, 1998.

[10] A.V. Oppenheim, R.W. Schafer, Discrete-Time Signal Processing, Prentice Hall, 2009.

[11] A. Ditkowski, A. Bhandari, B.W. Sheldon, Computing derivatives of noisy signals using orthogonal functions expansions, Journal of Scientific Computing 36 (3) (2008) 333–349.

[12] B. Augier, P. Bot, F. Hauville, M. Durand, Experimental validation of unsteady models for fluid structure interaction: application to yacht sails and rigs, Journal of Wind Engineering and Industrial Aerodynamics 101 (2012) 53–66.